FACULTY OF SCIENCE AND ENGINEERING

ASTROPHYSICS DEPARTMENT

BACHELOR RESEARCH PROJECT:

GRAVITATIONAL WAVES FROM INSPIRALLING BINARY NEUTRON STARS

A project submitted by Miquel Miravet for the Physics Bachelor in Groningen University

---

Supervised by:
Dr. Chris Van Den Broeck

Abstract

Neutron stars can be viewed as elastic objects to which one can associate resonant frequencies. As two neutron stars spiral towards each other, gravitational waves are emitted with a frequency that is monotonically increasing. When this frequency becomes equal to the resonant frequency of one of the neutron stars, the star briefly gets excited and undergoes oscillations, which take away orbital energy from the binary system.

The result is a sudden speed-up of the orbital motion, which gets imprinted upon the gravitational wave signal and is in principle observable, potentially yielding new information about the neutron star equation of state, that ultimately governs the effect. Though resonant excitations may not be observable with current gravitational wave detectors such as Advanced LIGO and Advanced Virgo, it is plausible that they will be visible with a planned next-generation observatory called Einstein Telescope. The aim of the project is to assess, using the Fisher matrix formalism, to what extent the effect can be seen. Therefore, the question one should ask is:

Are the resonant excitations in binary neutron star inspirals measurable with current and future gravitational wave detectors?

In order to get an answer to this question, one should analyze the errors in the parameter estimation of the inspiralling compact binary. Depending on the value of these errors and the parameter value, one can conclude whether or not certain parameters can be measurable in current and future gravitational wave detectors, such as Advanced LIGO, Advanced Virgo and Einstein Telescope.

Contents

Chapter 1

Introduction (Theoretical background)

The parameters which describe a gravitational wave can be found in its waveform. By solving Einstein equations from General Relativity and by approximating to linear order (which is valid for weak gravitational fields), one can get a perturbation over Minkowski's flat spacetime as a wave traveling through spacetime:

$$\Box\, \bar{h}_{\mu\nu} = -\frac{16\pi G}{c^4} T_{\mu\nu} \tag{1.1}$$

This perturbation is called **gravitational wave**.
Making use of the **transverse-traceless gauge** one can get a traveling plane wave with two polarizations in the z-direction:

$$h_{ij}^{TT} = \begin{pmatrix} h_+ & h_\times & 0 \\ h_\times & -h_+ & 0 \\ 0 & 0 & 0 \end{pmatrix}_{ij}$$

These components can be expressed in terms of the **mass quadrupole tensor**, which comes from the integration of the T^{00} component of the stress tensor:

$$M^{ij} = \frac{1}{c^2} \int d^3\mathbf{x} T^{00}(t, \mathbf{x}) x^i x^j \tag{1.2}$$

Hence:

$$h_+ = \frac{1}{r}\frac{G}{c^4}(\ddot{M}_{11} - \ddot{M}_{22}) \tag{1.3a}$$

$$h_\times = \frac{2}{r}\frac{G}{c^4}\, \ddot{M}_{12} \tag{1.3b}$$

Gravitational Waves from Coalescing Binaries. Taking two point particles orbiting around their center of mass with energy loss, the **mass quadrupole tensor** becomes:

$$M^{ij}(t) = \mu R(t)^2 \hat{e}^i(t)\hat{e}^j(t) \tag{1.4}$$

where μ is the *reduced mass* of the binary system and R is the separation distance between both point particles. The unit vector $\hat{e}(t)$ corresponds to the one that links the center of mass and the particle: $\hat{e}(t) = (\cos(\Phi(t)/2), \cos(\iota)\sin(\Phi(t)/2), \sin(\iota)\sin(\Phi(t)/2))$, where

$$\Phi(t) = \int_0^t dt' \omega_{gw}(t') \tag{1.5}$$

The rotation frequency of the particle is ω_{gw} and ι is the observation angle. Taking the time derivatives of (1.4) and inserting these results into eqs. (1.3):

$$h_+ = \frac{4}{r}\Big(\frac{G\mathcal{M}}{c^2}\Big)^{5/3}\Big(\frac{\pi f_{gw}(t_{ret})}{c}\Big)^{2/3}\frac{1+\cos^2(\iota)}{2}\cos(\Phi(t_{ret})) \tag{1.6a}$$

$$h_\times = \frac{4}{r}\Big(\frac{G\mathcal{M}}{c^2}\Big)^{5/3}\Big(\frac{\pi f_{gw}(t_{ret})}{c}\Big)^{2/3}\cos^2(\iota)\sin(\Phi(t_{ret})) \tag{1.6b}$$

where $\mathcal{M} \equiv \frac{(m_1 m_2)^{3/5}}{(m_1+m_2)^{1/5}}$ is called the **chirp mass** and it is really useful in gravitational-wave detection, rather than the real mass of the binary. The retarded time is given by t_{ret}; since the gravitational waves travel at the speed of light, the retarded time is the time when the wave begins to propagate from the point it is emitted to an observer. The gravitational-wave frequency $f_{gw}(t)$ has the expression:

$$f_{gw} = \frac{1}{\pi}\Big(\frac{G\mathcal{M}}{c^3}\Big)^{-5/8}\Big(\frac{5}{256}\frac{1}{\tau}\Big)^{3/8} \qquad \tau = t_{coal} - t \tag{1.7}$$

Detector response When a gravitational wave is detected, the measured strain is a linear projection of the arriving wave:

$$h(t) = F_+(\theta,\varphi,\phi)h_+(t) + F_\times(\theta,\varphi,\phi)h_\times(t)$$

The functions $F_+(\theta,\varphi,\phi)$ and $F_\times(\theta,\varphi,\phi)$ are the detector responses. They depend on the sky position (θ,ϕ) and the polarization angle of the gravitational wave, φ. Considering eqs. (1.6):

$$h(t) = A(t)\sqrt{F_+^2(1+\cos^2(\iota))^2 + F_\times^2 4\cos(\iota)}\cos(\Phi(t)+\phi_0) \tag{1.8}$$

with

$$\phi_0 = \arctan\left(\frac{-F_\times 2\cos(\iota)}{F_+(1+cos(\iota))}\right) \tag{1.9}$$

1.1 Stationary Phase Approximation (SPA)

For the calculations that follow the Fourier transform of the waveform is required:

$$\widetilde{h}\,(f) = \int_{-\infty}^{t_{coal}} h(t) e^{i2\pi ft} dt \tag{1.10}$$

where t_{coal} is the value of t when the coalescence takes place.

Normally, the complexity of the waveform is so high that an analytic Fourier expansion cannot be done. However, the **Stationary Phase Approximation** can be applied to get an analytic expression. Fourier transform:

$$\int_{-\infty}^{\infty} dt A(t) \cos(\Phi(t) + \phi_0) e^{2\pi ift} = \frac{1}{2} \int_{-\infty}^{\infty} dt A(t) \big(e^{i(\Phi(t)+\phi_0)} + e^{-i(\Phi(t)+\phi_0)}\big) e^{i2\pi ft} \tag{1.11}$$

$$\approx \frac{1}{2} e^{-i\phi_0} \int_{-\infty}^{\infty} dt A(t) e^{i(2\pi ft - \Phi(t))} \tag{1.12}$$

$e^{i(2\pi ft-\Phi(t))}$ is an unit vector in complex plane which can be expressed as: $e^{i\theta(t)}$. Due to the fact that the phase increases with time, for $2\pi ft + \Phi(t)$, the sum always grows. However, for $2\pi ft - \Phi(t)$, the difference grows and eventually becomes smaller. That means there is a stationary point.

$$\frac{d\theta}{dt} = 0 = 2\pi f - \dot{\Phi}\,(t) \Longrightarrow \dot{\Phi}\,(t_s) = 2\pi f$$

Expanding the exponent around the stationary point:

$$2\pi ft - \Phi(t) = 2\pi f t_s - \Phi(t_s) - \frac{1}{2}\,\ddot{\Phi}\,(t_s)(t - t_s)^2 + ...$$

A new variable can be defined: $x = \sqrt{\frac{\ddot{\Phi}(t_s)}{2}}(t - t_s)$. Thus, the integral is approximately equal to:

$$\frac{1}{2} A(t_s(f)) e^{-i\phi_0} e^{i(2\pi f t_s(f) - \Phi(t_s(f)))} \left(\frac{2}{\ddot{\Phi}\,(t_s(f))} \right) \int_{-\infty}^{\infty} dx e^{-ix^2}$$

The integrand is a Gaussian: $\int_{-\infty}^{\infty} dx e^{-ix^2} = \sqrt{\pi} e^{-i\pi/4}$. The final result is[1]:

$$\int dt A(t) \cos(\Phi(t) + \phi_0) e^{2\pi ift} \approx \frac{\sqrt{\pi}}{2} A(t(f)) e^{-i\phi_0} \left(\frac{2}{\ddot{\Phi}\,(t(f))} \right)^{1/2} e^{i\psi(f)},$$

where $\psi(f) = 2\pi f t(f) - \Phi(t(f)) - \frac{\pi}{4}$.

[1] In this case, only the 0-PN order is taken in determining the quadrupole expansion. In the PN expansion, more orders are considered.

Using the SPA (**stationary phase approximation**) and eqs.(1.5), (1.7) we have expressions for $\Phi(\tau)$ and hence $\ddot{\Phi}\ (\tau)$ where $\tau = t_{coal} - t$:

$$\Phi(t) = -2\left(\frac{5G\mathcal{M}}{c^3}\right)^{-5/8} \tau^{5/8}(t) + \Phi_c \tag{1.13}$$

Also:

$$t(f) = t_{coal} - \frac{5}{256}\Big(\frac{G\mathcal{M}}{c^3}\Big)^{-5/3}(\pi f)^{-8/3} \tag{1.14}$$

We finally end with a remarkable accurate approximation.[2]

$$\begin{aligned}\widetilde{h}\ (f) =& \sqrt{F_+^2(1+\cos^2(\iota))^2 + F_\times^2 4\cos(\iota)}\sqrt{\frac{5\pi}{96}}(\pi f)^{-7/6}\frac{c}{r}\Big(\frac{G\mathcal{M}}{c^3}\Big)^{5/6} \\ &\times exp\Big[i\Big(2\pi f t_{coal} - \Phi_{coal} + \frac{3}{4}\Big(\frac{8\pi G\mathcal{M}f}{c^3}\Big)^{-5/3} - \frac{\pi}{4}\Big)\Big]\end{aligned} \tag{1.15}$$

1.2 Fourier Domain Waveform for 3.5 PN Order

It is worth taking into account that in the previous section we have obtained the Fourier transform of the waveform for 0 PN-order, eq. (1.15). This is an expansion in powers of υ of the general-relativistic equation of motion for point particles in the center-of-mass frame. This Fourier domain waveform, which forms the basis of our further calculations, can be rewritten as

$$\widetilde{h}\ (f) = \mathcal{A}f^{-7/6}e^{i\varphi(f)} \tag{1.16}$$

where, remember from eq.(1.15), the amplitude $\mathcal{A} \propto \mathcal{M}^{5/6}Q(\text{angles})/r$. It is useful to deal with the *chirp mass*, $\mathcal{M} = \eta^{3/5}M$ in our calculations, rather than the total mass of the binary $M = m_1 + m_2$. The dimensionless *mass ratio* $\eta = m_1 m_2/M^2$ appears in many of the calculations as well.
The phase is given by

$$\varphi(f) = 2\pi f t_c - \phi_c - \frac{\pi}{4} + \frac{3}{128\eta\upsilon^5}\sum_{n=0}^{N}\alpha_n\upsilon^n \tag{1.17}$$

where υ is defined by $\upsilon = (\pi M f)^{1/3}$.

[2]By using the stationary phase approximation, the first binary neutron star merger was discovered.

The coefficients $\alpha_n, n = 0, ..., N$ (with N=7 in our study) that compose the Post-Newtonian expansion are given in Ref.[5] by

$$\alpha_0 = 1 \tag{1.18a}$$

$$\alpha_1 = 0 \tag{1.18b}$$

$$\alpha_2 = \Big[\frac{55}{9}\eta + \frac{3715}{756}\Big] \tag{1.18c}$$

$$\alpha_3 = \Big[4\beta - 16\pi\Big] \tag{1.18d}$$

$$\alpha_4 = \Big[\frac{3085}{72}\eta^2 + \frac{27145}{504}\eta + \frac{15293365}{508032} - 10\sigma\Big] \tag{1.18e}$$

$$\alpha_5 = \Big[\frac{38645\pi}{756} - \frac{65\pi}{9}\eta\Big](3\ln(\upsilon) + 1) \tag{1.18f}$$

$$\alpha_6 = \Big[-\frac{6848\gamma}{21} - \frac{127825}{1296}\eta^3 + \frac{76055}{1728}\eta^2 + \Big(\frac{2255\pi^2}{12} - \frac{15737765635}{3048192}\Big)\eta -$$

$$-\frac{640\pi^2}{3} + \frac{11583231236531}{4694215680} - \frac{6848\ln(4\upsilon)}{21}\Big] \tag{1.18g}$$

$$\alpha_7 = \pi\Big(\frac{77096675}{254016} + \frac{378515}{1512}\eta - \frac{74045}{756}\eta^2\Big) \tag{1.18h}$$

where

$$\beta = \frac{113}{12}\Big(\chi_s + \delta\chi_a - \frac{76\eta}{113}\chi_s\Big) \tag{1.19}$$

$$\sigma = \chi_a^2\Big(\frac{81}{16} - 20\eta\Big) + \frac{81\chi_s\chi_a\delta}{8} + \chi_s^2\Big(\frac{81}{16} - \frac{\eta}{4}\Big) \tag{1.20}$$

The symmetric and antisymmetric spins of the stars (χ_s, χ_a) have been already introduced in the coefficients of the Post-Newtonian expansion. We are going to study the addition of spins later on.

By dimensional regularisation λ and θ have been determined: $\lambda \cong -0.6451$ and $\theta \cong -1.28$ (*T. Damour, P. Jaranowski and G. Schäfer, Phys. Lett. B 513, 147 (2001)*).

One can see that the waveform depends on certain parameters, and a set of some of them will be made in order to estimate their errors:

$$\theta = \{\ln(\mathcal{A}), t_c, \phi_c, \ln(\mathcal{M}), \ln(\eta), \chi_s, \chi_a\} \tag{1.21}$$

where, remember, t_c is the coalescence time and ϕ_c refers to the phase at the moment of coalescence.

1.3 Mode Resonances in Coalescing Neutron Star Binaries

From now, let's consider that one of the neutron stars can be driven in resonance by the tidal force exerted by the other neutron star. These resonances can alter the wave signal emitted by the affected neutron star. Resonance may provoke a change in the phase of the waveform, which is thought that could bring potential information about the equation of state of the neutron star, or in other words, their internal structure.

Considering the resonant mode driving, it can be well described by two parameters, added to the previous set of parameters in order to analyze their errors. These parameters are the gravitational-wave frequency at which resonance occurs (f_0) and the phase shift parameter, $\Delta\Phi$. The resonant frequency f_0 is related to the resonant frequency: $f_0 = \frac{4}{3} f_{rot}$.

Consider the phase Φ including the resonance effect. We can assume that at early times $\Phi(t) = \Phi_{pp}(t)$, where $\Phi_{pp}(t)$ is the phase in (1.16), taking the neutron stars as point particles. After the resonance time, the phase shift is applied:

$$\Phi(t) = \begin{cases} \Phi_{pp}(t) & t \ll t_0 \\ \Phi_{pp}(t + \Delta t) - \Delta\Phi & t \gg t_0 \end{cases} \tag{1.22}$$

where t_0 is the time at which resonance occurs. To a good approximation we can express $\Delta\Phi$ as

$$\Delta\Phi = \dot{\Phi}_{pp}(t_0)\Delta t \tag{1.23}$$

Condition (1.23) means that resonance can be seen as an instantaneous change in frequency at $t = t_0$ with no corresponding intantaneous change in the phase. Inserting this expressing in eq.(1.22) and expanding to linear order in Δt, for late times:

$$\begin{aligned} \Phi(t) &= \Phi_{pp}(t) + \dot{\Phi}_{pp}(t)\Delta t - \dot{\Phi}_{pp}(t_0)\Delta t \\ &= \Phi_{pp}(t) + [\dot{\Phi}_{pp}(t) - \dot{\Phi}_{pp}(t_0)]\Delta t \\ &= \Phi_{pp}(t) + \left[\frac{\dot{\Phi}_{pp}(t)}{\dot{\Phi}_{pp}(t_0)} - 1\right]\dot{\Phi}_{pp}(t_0)\Delta t \end{aligned} \tag{1.24}$$

Using the expression (1.23) and $\dot{\Phi}_{pp}(t) = 2\omega$:

$$\Phi(t) = \Phi_{pp}(t) + \left[\frac{\omega(t)}{\omega(t_0)} - 1\right]\Delta\Phi \tag{1.25}$$

If one looks at this expression, it can be seen that the phase perturbation grows with time after the resonance. Alternatively, we can set the phase perturbation to a non-zero value before the resonance. It can be done by defining a new point-particle waveform phase $\widetilde{\Phi}_{pp}$:

$$\widetilde{\Phi}_{pp} \equiv \Phi_{pp}(t + \Delta t) - \Delta\Phi \tag{1.26}$$

We have used different conventions for the starting time and starting phase. Finally, using $\omega = 2\pi f$ and the **stationary phase approximation**:

$$\Phi(f) = \begin{cases} \Phi_{pp}(f) + (1 - f/f_0)\Delta\Phi & f_0 - f \gg \Delta f_{res} \\ \Phi_{pp}(f) & f - f_0 \gg \Delta f_{res} \end{cases} \tag{1.27}$$

However, Δf_{res}, which is the bandwidth of the resonance, is small enough to be neglected. Eq.(1.27) is rewritten as

$$\Phi(f) = \begin{cases} \Phi_{pp}(f) + (1 - f/f_0)\Delta\Phi & f \leq f_0 \\ \Phi_{pp}(f) & f > f_0 \end{cases} \tag{1.28}$$

Regarding eq.(1.28), the phase perturbation due to the resonant mode driving is simply a linear function of frequency, achieving the maximum value of $\Delta\Phi$. With the aim of detecting this phase shift, it should be considerably larger than unity. From Ref.[4], when considering the resonant (*r-modes*), the phase shift is small compared to unity. The only way to have $\Delta\Phi \geq 1$ is only possible for spin frequencies of order several hundred Hz, which we will see in the next subsection it is unlikely for most neutron star inspiralling binaries. Taking into account the resonances, the new parameter-vector should be

$$\theta = \{\ln(\mathcal{A}), t_c, \phi_c, \ln(\mathcal{M}), \ln(\eta), \chi_s, \chi_a, f_0, \Delta\Phi\} \tag{1.29}$$

1.4 Addition of Spin to Parameter Estimation

The next step in the study of the gravitational-wave emission from a neutron star binary is the addition of the spin question. Most of the observed neutron stars are found to be weakly spinning. There is a theoretical upper limit on the spin rate beyond which the neutron star is gravitationally unstable: $||\mathbf{S}||/m^2 \sim 0.7$ (Ref.[5]).

Since spins are really close to zero, somebody can suppose that $\chi_1 = \chi_2 = 0$. However, if one wants to be completely physically consistent, we should consider the spin of one of the neutron stars to be non-zero (the star which undergoes resonance). χ_1 can be expressed as:

$$\chi_1 = \frac{c}{G}\frac{J_1}{m_1^2} = \frac{c}{G}\frac{I_1\omega_{rot}}{m_1^2} \tag{1.30}$$

The moment of inertia can be the moment of a sphere: $I = \frac{2}{5}mR^2$, where m is the neutron star mass and R is the neutron star radius. They are set to be $1.4M_\odot$ and 10 km, respectively. Then, substituting f_{rot} in terms of f_0 and the moment of inertia in expression (1.30), one has:

$$\chi_1(f_0) = \frac{c}{G}\frac{2}{5}m_1R^2\frac{3}{4}\frac{2\pi f_0}{m_1^2} \tag{1.31}$$

which explicitly depends on f_0. In order to introduce the spin, two more parameters are added to the template we already had from the previous analysis. The spin variables χ_s (symmetric) and χ_a (anti-symmetric) are related to the spin vectors as:

$$\chi_s = \frac{\chi_1 + \chi_2}{2} \qquad \chi_a = \frac{\chi_1 - \chi_2}{2} \tag{1.32}$$

Chapter 2

Parameter Estimation: Fisher Matrix Formalism

2.1 Matched Filtering

There exist some different methods suggested for the detection of gravitational waves from inspiralling binaries, but matched filtering is the most recommended one.

2.1.1 Digging a signal out of noise

This is a classical problem in physics. We will see that values of $h(t)$ much smaller than noise can be detected if the shape of $h(t)$ is known, at least to some level of accuracy.
When a gravitational wave is detected, the measured strain is composed of noise and the signal:

$$s(t) = n(t) + h(t)$$

Noise can appear due to seismic vibrations or Brownian motion, among others. The shape of the signal is assumed to be approximately known. The waveform is integrated against the output $s(t)$ over an observation time T:

$$\frac{1}{T}\int_0^T dt s(t)h(t) = \frac{1}{T}\int_0^T dt n(t)h(t) + \frac{1}{T}\int_0^T dt h^2(t) \tag{2.1}$$

$h(t)$ and $s(t)$ are oscillatory functions. The second integrand of the previous equation is positive definite: it grows during the observation time. Its average value should be then

$$\frac{1}{T}\int_0^T dt h^2(t) \sim h_0^2 \tag{2.2}$$

where h_0 is the characteristic amplitude of the waveform. Since the noise and the signal are not correlated, the product $n(t)h(t)$ will be still oscillating. The integral will be dimensionless after adding a typical characteristic time, τ_0:

$$\frac{1}{T}\int_0^T dt h(t)n(t) \sim \left(\frac{\tau_0}{T}\right)^{1/2} n_0 h_0 \tag{2.3}$$

To detect the signal given by (2.2) against the background given by (2.3), there's no need of having $h_0 > n_0$, it is enough having $h_0^2 > \left(\frac{\tau_0}{T}\right)^{1/2} n_0 h_0$. Thus, in the limit of $T \to \infty$, the term given in (2.3) goes to 0, and the noise contribution would have been filtered out. However, this is not a realistic situation.

2.1.2 Matched Filtering

Matched filtering consists of passing the input data $s(t)$ of the detector through a linear filter $K(t)$ constructed from the expected signal $h(t;\theta)$, where θ is the vector given in (1.21). We define:

$$\hat{s} = \int_{-\infty}^{+\infty} dt s(t) K(t) \tag{2.4}$$

Define S as the expected value of the quantity defined above when a signal $h(t)$ is present, and N will be the *rms* value when no signal is in the detector:

$$\begin{aligned} S &= \int_{-\infty}^{+\infty} dt \langle s \rangle K(t) \\ &= \int_{-\infty}^{+\infty} df \, \tilde{h}\,(f) K^*(f) \end{aligned} \tag{2.5}$$

since $\langle n(t) \rangle = 0$, because noise is considered Gaussian and stationary. Furthermore:

$$\begin{aligned} N &= [\langle \hat{s}^2 \rangle - \langle \hat{s} \rangle^2]_{h=0}^{1/2} \\ &= [\langle \hat{s}^2 \rangle]_{h=0}^{1/2} \\ &= \Big[\int_{-\infty}^{+\infty} dt \int_{-\infty}^{+\infty} dt' \langle n(t) n(t') \rangle K(t) K(t') \Big]^{1/2} \\ &= \Big[\int_{-\infty}^{+\infty} df \frac{1}{2} S_n(f) |\tilde{K}^*\,(f)|^2 \Big]^{1/2} \end{aligned} \tag{2.6}$$

where $S_n(f)$ is called the **noise power spectral density (PSD)** and is defined as

$$\langle \tilde{n}^*\,(f)\, \tilde{n}\,(f') \rangle = \frac{1}{2} \delta(f - f') S_n(f) \tag{2.7}$$

The noise power spectral density can be seen as the variance of noise as a function of the frequency and is given by the detector.

2.1.3 Signal-to-noise ratio

Define **signal-to-noise ratio**:

$$\frac{S}{N} = \frac{\langle \hat{s} \rangle_h}{\left[\langle \hat{s}^2 \rangle - \langle \hat{s} \rangle^2 \right]_{h=0}^{1/2}} \tag{2.8}$$

This quantity shows how strong the detected signal is and which level of noise we have in the detector. The larger the SNR, the louder the signal in the detector. The most important goal is **finding out which filter** $K(t)$ **maximizes S/N**. Using expressions of S and N obtained before, one arrives at:

$$\frac{S}{N} = \frac{\int_{-\infty}^{+\infty} df\ \widetilde{h}\ (f) K^*(f)}{\left[\int_{-\infty}^{+\infty} df \frac{1}{2} S_n(f) |\widetilde{K^*}\ (f)|^2 \right]^{1/2}}$$

Defining the **noise-weighted inner product**:

$$(A|B) = 4\mathbb{R} \int_0^{\infty} df \frac{\widetilde{A^*}\ (f)\ \widetilde{B}\ (f)}{S_n(f)}$$

Therefore, S/N can be rewritten as:

$$\frac{S}{N} = \frac{(\mathbf{K}|h)}{(\mathbf{K}|\mathbf{K})^{1/2}} \qquad \mathbf{K} = \frac{1}{2} S_n(f)\ \widetilde{K}\ (f)$$

Signal-to-noise ratio can also be expressed as the inner product between an unit vector and the waveform:

$$\frac{S}{N} = (\hat{\mathbf{K}}|h) \qquad \hat{\mathbf{K}} = \frac{\mathbf{K}}{(\mathbf{K}|\mathbf{K})^{1/2}}$$

It is easy to see that in order to maximise S/N, $\hat{\mathbf{K}} \propto h \rightarrow \mathbf{K} \propto h$, which leads to:

$$\frac{S}{N} = \sqrt{(h|h)} \tag{2.9}$$

that is[1]

$$\left(\frac{S}{N}\right)^2 = 4 \int_0^{\infty} df \frac{|\ \widetilde{h}\ (f)|^2}{S_n(f)} \tag{2.10}$$

[1]Even though the upper limit of the integral is infinite, we will use instead the value $f_lso = (6^{3/2}\pi M)^{-1}$, which is the frequency of the last stable orbit of the binary system, when the signal shuts off. Moreover, instead of having 0 for the lower limit of the integral, we will use the lower cut-off frequency f_s given by the noise PSD.

In reality, we must consider many different trial waveforms h_i. We can apply an optimal filter ($\hat{\mathbf{K}}_i \propto h_i$) to the data:

$$\left(\frac{S}{N}\right)_i = (\hat{\mathbf{K}}_i)|\langle s\rangle) \tag{2.11}$$

$$= \frac{(\mathbf{K}_i|\langle s\rangle)}{\sqrt{(\mathbf{K}_i|\mathbf{K}_i)}} \tag{2.12}$$

$$= \frac{(h_i|\langle s\rangle)}{\sqrt{(h_i|h_i)}} \tag{2.13}$$

Since in practice we only know the detected signal and not its expectation value:

$$\left(\frac{S}{N}\right)_i = \frac{(h_i|s)}{\sqrt{(h_i|h_i)}} \tag{2.14}$$

Therefore, we must find the maximum of the signal-to-noise ratio over a given template bank, $\overline{\theta}$:

$$\left(\frac{S}{N}\right)_{max} = \overset{max}{i} \frac{(h(\overline{\theta}_i|s))}{\sqrt{(h(\overline{\theta}_i|h(\overline{\theta}_i)}} \tag{2.15}$$

2.2 Fisher Matrix Formalism

Even though there is prior knowledge of the waveform, we do not know anything about its parameters. We need to find the **posterior probability density**:

$$p(\overline{\theta}|d, \mathcal{H})$$

where $\overline{\theta}$ are the parameters, $\mathcal{H}$ is the hypothesis and d(t) is the data composed of the noise and the signal.
Using Bayes' theorem:

$$p(\overline{\theta}|d, \mathcal{H}) = \frac{p(d|\overline{\theta}, \mathcal{H})p(\overline{\theta}|\mathcal{H})}{p(d|\mathcal{H})} \tag{2.16}$$

The evidence $p(d|\mathcal{H})$ is set to be a normalization constant. The prior probability density $p(\overline{\theta}|\mathcal{H})$ is a function we choose ourselves, based on what we know before the measurements. Therefore, we assume an uniform prior: $p(\overline{\theta}|\mathcal{H})$= constant. We end with:

$$p(\overline{\theta}|d, \mathcal{H}) \propto p(d|\overline{\theta}, \mathcal{H}) \tag{2.17}$$

that is, the posterior probability density is proportional to the likelihood. In the likelihood density, the hypothesis and the parameter values are assumed known ($h(\overline{\theta}; t)$ is assumed known), so we have a probability distribution for the noise, since $d(t) = n(t) + h(\overline{\theta}; t)$.
Assuming an stationary and gaussian noise, the probability for noise realization as a whole:

$$p[n] = \prod_{i=1}^{N} p(\widetilde{n}_i) = \mathcal{N} e^{-\frac{1}{2}\sum_{i=1}^{N} \frac{|\widetilde{n}_i|^2}{\sigma_i^2}} \tag{2.18}$$

It is convenient to take the continuum limit:

$$p[n] = \mathcal{N} e^{-\frac{1}{2}\sum_{i=1}^{N} \frac{|\widetilde{n}_i|^2}{\sigma_i^2 \Delta f} \Delta f} \longrightarrow \mathcal{N} e^{-\int_{-\infty}^{\infty} \frac{|\widetilde{n}(f)|}{S_n(f)} df} \tag{2.19}$$

The variance is related to the noise power spectral density [2]:

$$\sigma_i^2 \to \delta(f' - f)\frac{1}{2} S_n(f) \tag{2.20}$$

where $\delta(f' - f) \sim \frac{1}{\Delta f}$. The previous integral from eq.(2.19) can be expressed in terms of the noise-weighted inner product:

$$(m|n) \equiv 2 \int_0^{\infty} df \frac{\widetilde{m}^* (f)\, \widetilde{n}\, (f) + \widetilde{n}^* (f)\, \widetilde{m}\, (f)}{S_n(f)} \tag{2.21}$$

We end with:

$$p(\overline{\theta}|d, \mathcal{H}) = \mathcal{N} e^{-\frac{1}{2}(d - h(\overline{\theta})|d - h(\overline{\theta}))} \tag{2.22}$$

since $\widetilde{n}\, (f) = \widetilde{d}\, (f) - \widetilde{h}\, (\overline{\theta}; f)$. For the exponent:

$$(d - h|d - h) = -2(d|h) + (h|h) + const. \tag{2.23}$$

where $(d|d)$ is set to be constant. Then:

$$p(\overline{\theta}|d, \mathcal{H}) = \mathcal{N}' e^{+(d|h) - \frac{1}{2}(h|h)} \tag{2.24}$$

Let's express the measured values as

$$\overline{\theta} = \overline{\theta}_{ML} + \delta\overline{\theta} \tag{2.25}$$

ML means "Maximum Likelihood", i.e. the point where the likelihood probability $p(\overline{\theta}|d, \mathcal{H})$ peaks. It is also assumed that $\overline{\theta}_{ML} = \overline{\theta}_{real}$. Therefore, we can apply the logarithm to the likelihood

$$\log p(\overline{\theta}|d, \mathcal{H}) = (d|h) - \frac{1}{2}(h|h) + const. \tag{2.26}$$

and determine its derivative w.r.t. any parameter "θ_i" at the ML point (maximum):

$$0 = \frac{\partial}{\partial \theta^i} \log p(\overline{\theta}|d, \mathcal{H})\, |_{ML} = \left(d \mid \frac{\partial h}{\partial \theta^i}\right) |_{ML} - \left(h \mid \frac{\partial h}{\partial \theta^i}\right) |_{ML} = 0 \tag{2.27}$$

[2] Remember from expression (2.7): $\langle \widetilde{n} *(f)\, \widetilde{n}\, (f') \rangle = \frac{1}{2}\delta(f' - f) S_n(f)$

The signal can be expanded around the maximum likelihood values:

$$h(\overline{\theta}) = h(\overline{\theta}_{ML}) + \frac{\partial h}{\partial \theta^i} \mid_{ML} \delta\theta^i + \frac{1}{2}\frac{\partial^2 h}{\partial\theta^i\partial\theta^j}\delta\theta^i\delta\theta^j \tag{2.28}$$

where we have used the Einstein summation convention. The exponent of eq.(2.24) can be rewritten as:

$$\begin{aligned}(d|h) - \frac{1}{2}(h|h) = (d|h) \mid_{ML} &+ \Big(d \mid \frac{\partial h}{\partial\theta^i}\Big) \mid_{ML} \delta\theta^i \\ &+ \frac{1}{2}\Big(d \mid \frac{\partial^2 h}{\partial\theta^i\partial\theta^j}\Big) \mid_{ML} \delta\theta^i\delta\theta^j \\ &- \frac{1}{2}(h|h) \mid_{ML} - \Big(h \mid \frac{\partial h}{\partial\theta^i}\Big) \mid_{ML} \delta\theta^i \\ &- \frac{1}{2}\Big(h \mid \frac{\partial^2 h}{\partial\theta^i\partial\theta^j}\Big) \mid_{ML} \delta\theta^i\delta\theta^j \\ &- \frac{1}{2}\Big(\frac{\partial h}{\partial\theta^i} \mid \frac{\partial h}{\partial\theta^j}\Big) \mid_{ML} \delta\theta^i\delta\theta^j \end{aligned} \tag{2.29}$$

The terms which are not dependent on $\delta\overline{\theta}$ are set to be constant, and two other terms vanish due to the expression in eq.(2.27). Therefore, the final expression of the exponent is:

$$\begin{aligned}(d|h) - \frac{1}{2}(h|h) &= \frac{1}{2}\Big(d - h \mid \frac{\partial^2 h}{\partial\theta^i\partial\theta^j}\Big) \mid_{ML} \delta\theta^i\delta\theta^j \\ &- \frac{1}{2}\Big(\frac{\partial h}{\partial\theta^i} \mid \frac{\partial h}{\partial\theta^j}\Big) \mid_{ML} \delta\theta^i\delta\theta^j \\ &= \frac{1}{2}\Big(n \mid \frac{\partial^2 h}{\partial\theta^i\partial\theta^j}\Big) \mid_{ML} \delta\theta^i\delta\theta^j \\ &- \frac{1}{2}\Big(\frac{\partial h}{\partial\theta^i} \mid \frac{\partial h}{\partial\theta^j}\Big) \mid_{ML} \delta\theta^i\delta\theta^j \end{aligned} \tag{2.30}$$

The first term involving noise is negligible compared to the second term, due to the fact that the derivatives of the signal have much more correlation between them than noise and signal. Defining the Fisher matrix coefficients $\Gamma_{ij} \equiv \Big(\frac{\partial h}{\partial\theta^i} \mid \frac{\partial h}{\partial\theta^j}\Big) \mid_{ML}$, the errors in the parameter estimation obey a Gaussian probability distribution of the form

$$p(\delta\theta|d,\mathcal{H}) = \mathcal{N}'' e^{-\frac{1}{2}\Gamma_{ij}\delta\theta^i\delta\theta^j} \tag{2.31}$$

with [3]

$$\Gamma_{ij} \equiv (h_i|h_j) = 2\int_0^\infty df \frac{\tilde{h}_i^*(f)\,\tilde{h}_j(f) + \tilde{h}_i^*(f)\,\tilde{h}_j(f)}{S_n(f)} \tag{2.32}$$

[3] Again, even though the upper limit of the integral is infinite, we will use instead the value f_lso. For the lower limit of the integral, we will use the lower cut-off frequency f_s as well.

We are interested in the 1-sigma spread of $\delta\overline{\theta}$: $\Delta\theta_i = \sqrt{\langle(\delta\theta_i)^2\rangle}$. Firstly, we can consider 1 parameter to analyse:

$$p[\delta\theta] \approx \mathcal{N} e^{-\frac{1}{2}\Gamma\delta\theta^2} \approx \mathcal{N} e^{-\frac{1}{2}\frac{\delta\theta^2}{\sigma^2}} \tag{2.33}$$

where $\sigma = \sqrt{\Gamma^{-1}}$. Now, Γ is a number.
Therefore, the 1-sigma uncertainty $\Delta\theta$ will be:

$$\Delta\theta^2 \equiv \langle(\delta\theta)^2\rangle = \Gamma^{-1} \tag{2.34}$$

Generalizing to multiple parameters, we must define the **variance-covariance matrix**, which is simply the inverse of the Fisher matrix:

$$\Sigma^{ij} \equiv \langle\Delta\theta^i\Delta\theta^j\rangle = (\Gamma^{-1})^{ij} \tag{2.35}$$

We are interested in its diagonal, which contains the *rms* errors[4] of the parameters that have been studied:

$$\sigma^i = \sqrt{\Sigma^{ii}} \tag{2.36}$$

The aim of this project is to study the parameters given in (1.29), by obtaining the Fisher matrix (2.32) and their *rms* errors. The calculation will allow determining whether or not it could be possible to detect the $\Delta\Phi$, which may allow getting some information about the internal structure of neutron stars.

[4]In the diagonal elements the correlations between the parameters introduced in the Fisher matrix are taken into account.

Chapter 3

Results

In this chapter, all the concepts introduced before will be applied to show how the procedure works. For all the steps, the chosen *masses of the neutron stars* will be $m_1 = m_2 = 1.4M_\odot$. Values for the parameters given in (1.29) are:

$$
\begin{aligned}
t_c &= 0 \text{ s} \\
\phi_c &= 0 \text{ rads} \\
f_0 &= 16 \text{ Hz} \\
\Delta\Phi &= 1 \text{ rads}
\end{aligned}
$$

3.1 Neutron Stars as point particles

When considering neutron stars as point particles, don't care about resonances. The parameters studied in this section are the ones given in (1.21). It is proper to set the noise PSD from the calculation of Fisher coefficients. For this first step, the noise PSD corresponds to a fit of advanced LIGO detector:

$$
S_n(f) = \begin{cases} S_0\left[x^{-4.14} - 5x^{-2} + \frac{111(1-x^2+x^4/2)}{(1+x^2/2)}\right] & f \geq f_s \\ \\ \infty & f < f_s \end{cases} \tag{3.1}
$$

Here $x = f/f_0$, $f_0 = 215$ Hz, $S_0 = 10^{-49}\ Hz^{-1}$ and the lower cutoff frequency $f_s = 20$ Hz.

Using this noise PSD to calculate the Fisher matrix coefficients and the covariant matrix making use of expressions (2.32) and (2.35), respectively, we can get the different values of the root-mean-square errors for the parameters already shown. The waveform that one can take is the given in (1.16).

In order to show how the results evolve in the Post-Newtonian expansion, the calculation can be done from 1 PN to 3.5 PN, in steps of 0.5 PN. Another thing to say is that the amplitude of the waveform is fixed by an SNR of 10. Using (2.10) and setting $\frac{S}{N} = 10$, it is easy to find that $A = 2.318 \times 10^{-22}\ s^{-1/6}$.

	Errors			
PN order	Δt_c	$\Delta\phi_c$	$\frac{\Delta\mathcal{M}}{\mathcal{M}}$	$\frac{\Delta\eta}{\eta}$
1PN	0.3983	0.9268	0.0274%	4.377%
1.5PN	0.4676	1.476	0.0146%	1.653%
2PN	0.4631	1.393	0.0147%	1.782%
2.5PN	0.5103	1.358	0.0137%	1.344%
3PN	0.4326	1.469	0.0148%	1.725%
3.5PN	0.4970	1.145	0.0142%	1.563%

Table 1: Parameter errors from 1PN to 3.5PN for a NS-NS binary system.The noise power spectral density (PSD) corresponds to advanced LIGO detector. For the results, Δt_c is in miliseconds, and $\Delta\phi_c$ is in radians.

These results are shown in order to make clear that the computer code is robust enough. Considering neutron stars as point particles does not have any physical meaning and we are not interested in the previous results. The following table is taken from Ref.[2] to check that the code we are using is correct:

	NS-NS			
PN Order	Δt_c	$\Delta\phi_c$	$\Delta\mathcal{M}/\mathcal{M}$	$\Delta\eta/\eta$
Advanced LIGO				
1PN	0.3977	0.9256	0.0267%	4.656%
1.5PN	0.4668	1.474	0.0142%	1.638%
2PN	0.4623	1.392	0.0143%	1.764%
2.5PN	0.5090	1.359	0.0134%	1.334%
3PN	0.4938	1.331	0.0135%	1.348%
3.5PN	0.5193	1.279	0.0133%	1.319%

Table 2: Parameter errors from 1PN to 3.5PN for the same system as in Table 1. These results come from Ref.[2].

3.2 Spin Addition

When adding spins to the neutron stars, the values of the rms errors are supposed to change a bit. The parameters we are interested in are the resonant frequency f_0 and the change of phase $\Delta\Phi$. It is interesting to compare the data by using different noise PSD, one for advanced LIGO and the other for the Einstein Telescope (ET). An updated version of the advanced LIGO's noise PSD is:

$$S_n(f) = \begin{cases} 10^{-48}(0.0152x^{-4} + 0.2935x^{9/4} + 2.7951x^{3/2} - \\ -6.5080x^{3/4} + 17.7622) & f \geq f_s \\ \\ \infty & f < f_s \end{cases} \tag{3.2}$$

Here, $x = f/245.4$ and the low-frequency cutoff is again $f_s = 20$ Hz. The noise PSD corresponding to ET is a numerical fitting calculated with Mathematica.

Furthermore, instead of fixing the SNR to 10, the distance is fixed now to $d = 50$ Mpc. Using eq. (1.15), and setting the source "face-on" or "face-off" ($\iota = 0$ or $\iota = \pi$) and at zenith or nadir ($\theta = 0$ or $\theta = \pi$), one can get a larger SNR and an amplitude given by

$$A = \sqrt{\frac{5\pi}{24}}\pi^{-7/6}\left(\frac{1}{d}\right)\mathcal{M}^{5/6}. \tag{3.3}$$

It is also useful to know that the average over sky position and orientation gives an SNR equal to $\rho_{ave} = \frac{2}{5}\rho_{best}$. Thus, if one wants to get the parameter uncertainty estimates for the average case, it only has to multiply the values obtained with the amplitude from (3.3) by a factor of $\frac{5}{2}$.

Taking $\chi_s = \chi_a = \chi_1/2$ in this case, one can make some plots to study their trends when f_0 and $\Delta\Phi$ are changed. Values of f_0 are taken from 100 Hz to 1000 Hz in steps of 10 Hz, with $\Delta\Phi = 2\pi$ rads.

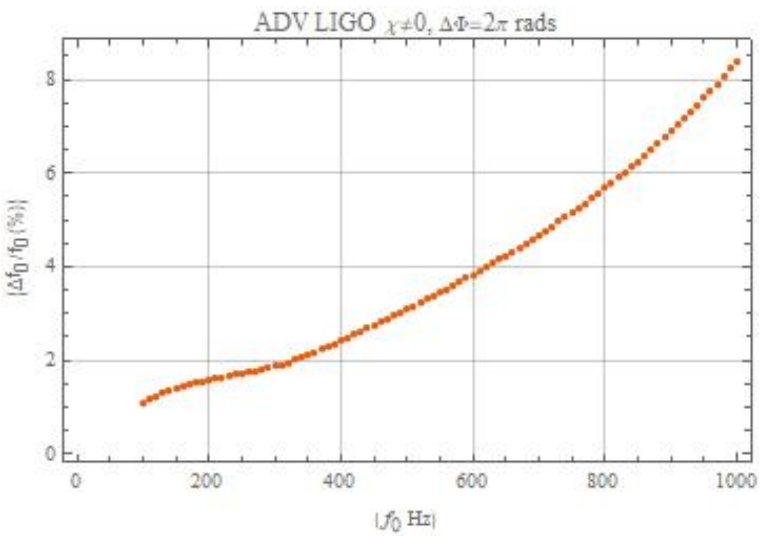

Figure 1: Absolute error value of f_0 (as a percentage) as a function of the resonant frequency, f_0. The noise PSD is given in eq.(3.2) for ADV LIGO.

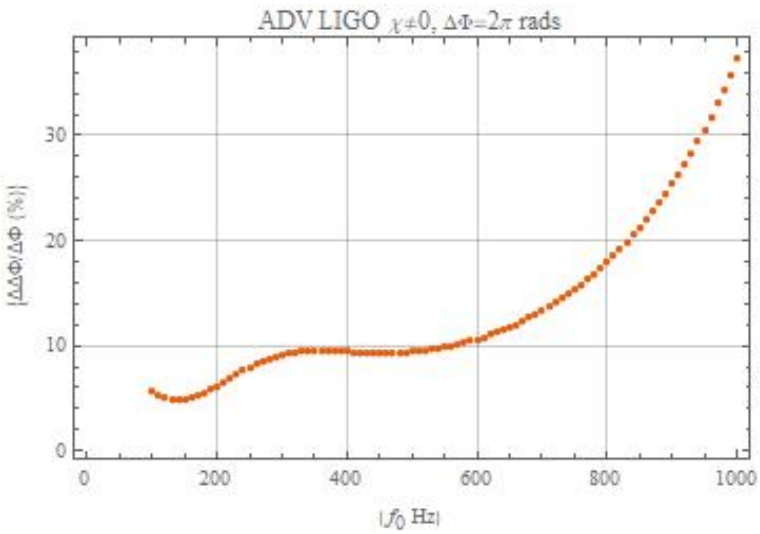

Figure 2,: Absolute error of $\Delta\Phi$ (as a percentage) as a function of the resonant frequency, f_0 for Advanced LIGO.

Let's check now how the plots look by using the ET's noise PSD:

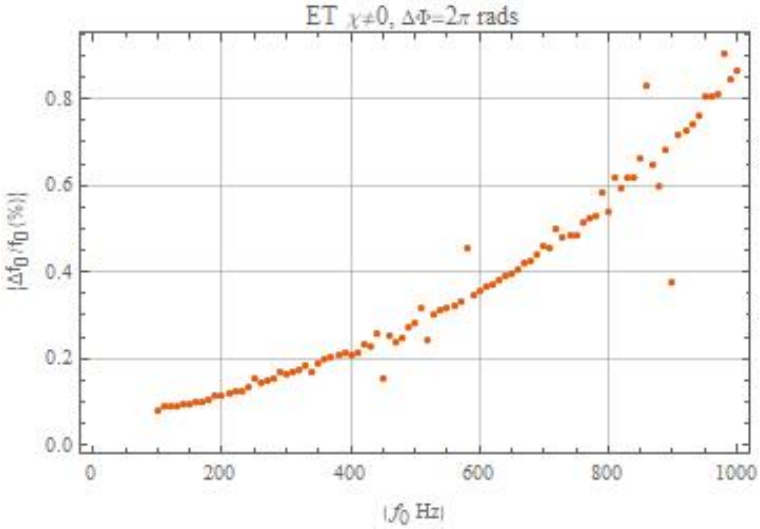

Figure 3: Absolute error value of f_0 (as a percentage) as a function of the resonant frequency, f_0. The noise PSD corresponds to Einstein Telescope.

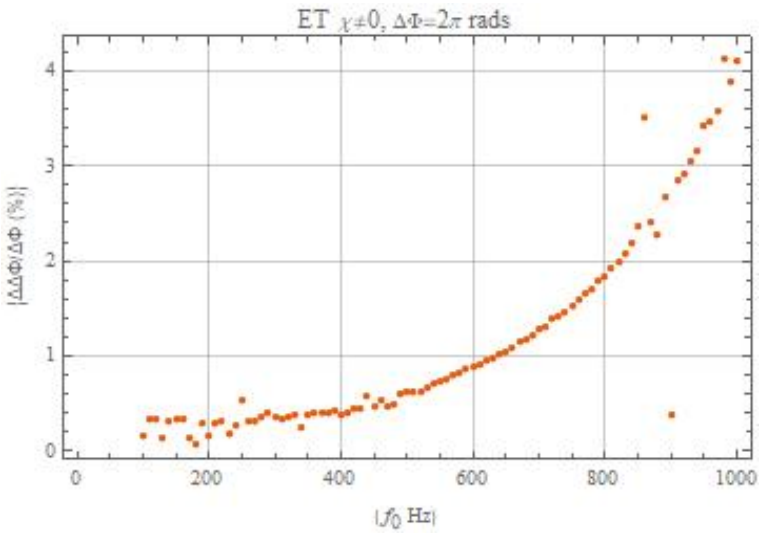

Figure 4: Absolute error value of $\Delta\Phi$ (as a percentage) as a function of the resonant frequency, f_0. The noise PSD corresponds to Einstein Telescope.

It is also worth showing how Δf_0 and $\Delta(\Delta\Phi)$ depend on $\Delta\Phi$. To do that, we take values of $\Delta\Phi$ from 0 rads to 2π rads, and a fixed resonant frequency, $f_0 = 100$ Hz. Regarding advanced LIGO results:

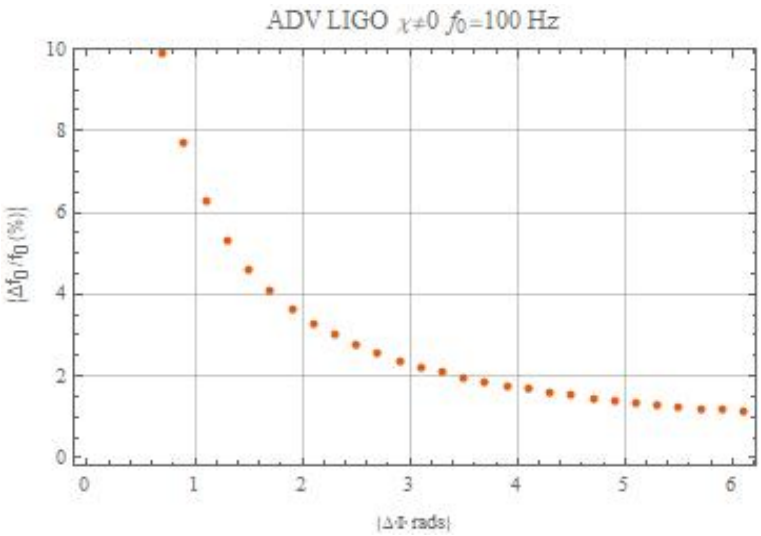

Figure 5: Absolute error value of f_0 (as a percentage) as a function of the phase shift $\Delta\Phi$. The noise PSD is given in eq.(3.2) for ADV LIGO.

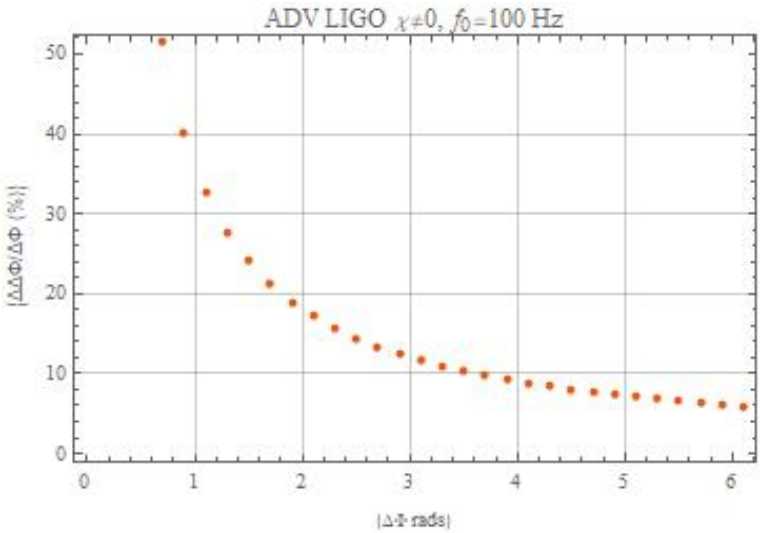

Figure 6: Absolute error value of $\Delta\Phi$ (as a percentage) as a function of the phase shift $\Delta\Phi$. The noise PSD corresponds to the ADV LIGO.

Now, the results for Einstein Telescope:

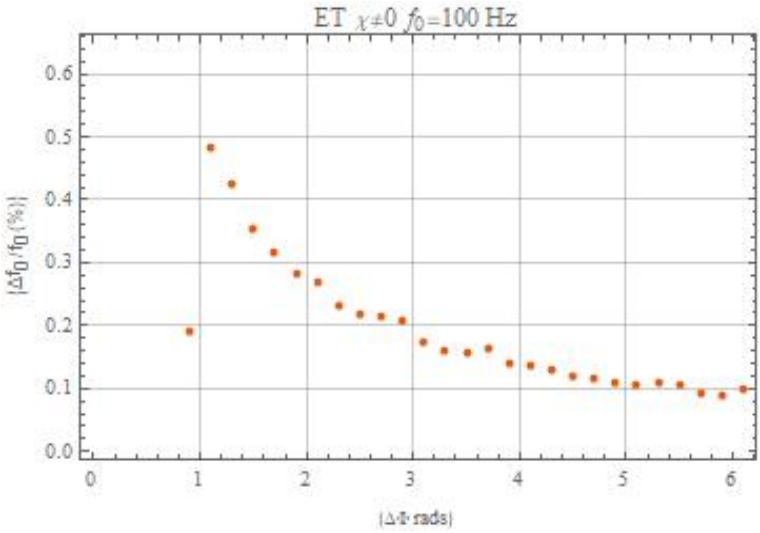

Figure 7: Absolute error value of f_0 (as a percentage) as a function of the phase shift $\Delta\Phi$. The noise PSD corresponds to Einstein Telescope.

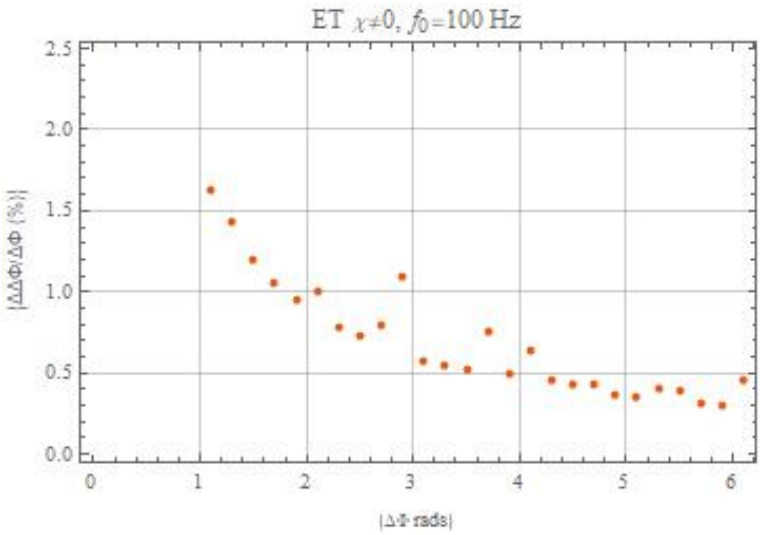

Figure 8: Absolute error value of $\Delta\Phi$ (as a percentage) as a function of the phase shift $\Delta\Phi$. The noise PSD corresponds to Einstein Telescope.

Chapter 4

Analysis of Results and Conclusions

Since the aim of the project is to analyze the most realistic case of a neutron star binary system, the situation in which neutron stars are point particles is only used to check whether or not the results are similar to the ones of Ref.[2].

When resonance is added, the Fisher matrix becomes bigger and a bit more realistic. One should keep in mind that resonance is only possible for the spinning case, that is why it is not necessary to show the plots for the non-spinning situation, since they are not physically realistic. It is quite interesting to explain the general trends of the plots.

Fixed phase shift. The general behaviour of this plots is that, for high resonant frequencies, errors increase. It can be seen with the noise PSD, which goes up at higher frequencies. This means that noise blows up.

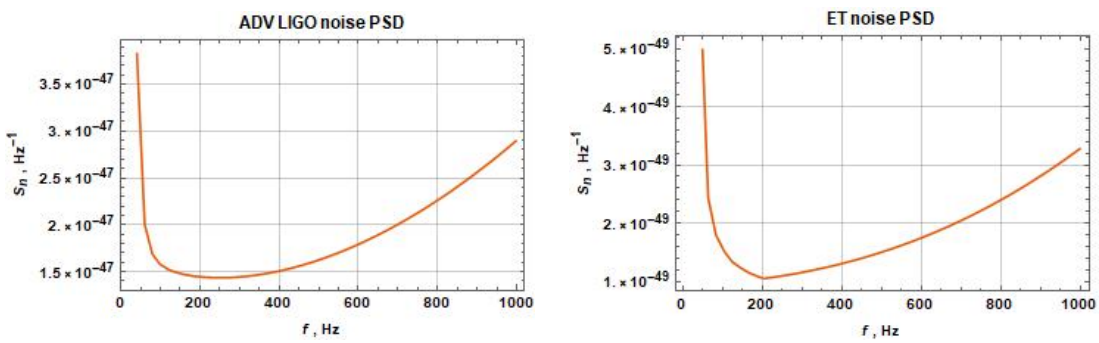

Figure 9: Plots of the noise PSD's, the first introduced in (3.2) for ADV LIGO and the second corresponds to ET. One can notice that the values of the PSD in the case of the Einstein Telescope are 100 times lower, that is why Einstein Telescope is more sensitive.

Fixed resonant frequency. The general trend is that, as $\Delta\Phi$ increases, the absolute error of the phase shift decreases, and the same for the resonant frequency. The reason for this trend is that since $f_0 = 100$ Hz is the frequency at which the detector is more sensitive, increasing resonance effect should make resonance parameters easier to detect, such as f_0 and $\Delta\Phi$.

In Advanced LIGO's case, the shape seems quite regular, but this is not the case for ET's plots, where some points do not behave properly. It seems that numerical errors arise when it comes to the numerical inversion of the Fisher matrix. One way to check the invertibility of the Fisher matrix is to multiply it by the covariance matrix and see if the product is equal to the identity matrix, or a least close to it.

$$\Gamma\Sigma = I + \epsilon \tag{4.1}$$

A more sophisticated way to check the invertibility of the Fisher matrix to make use of the **singular value decomposition**. By checking the Fisher matrix's eigenvalues, one can see how invertible it is. If they are close to zero, it directly means that it is badly invertible, and the covariant matrix would contain some numerical errors. We can do the analysis of the invertibility, for example, of one case, let's say $\left(\frac{\Delta(\Delta\Phi)}{\Delta\Phi}\right)$ vs f_0.

f_0	Eigenvalues, λ							
250	4.455×10^{23}	9.537×10^{14}	5.111×10^{11}	1.636×10^{9}	185200	17290	12.31	0.1008
900	2.512×10^{24}	9.449×10^{14}	5.113×10^{11}	1.572×10^{9}	247500	6816	2.387	0.3796
600	5.550×10^{24}	9.373×10^{14}	5.118×10^{11}	1.538×10^{9}	275400	1362	-2.306	2.122

Table 3: Eigenvalues of Fisher matrix for the ET with $\chi_1 \neq 0$, given some values of f_0 in Hz.

Here the last two eigenvalues are quite close to zero, especially the last one. The highest and lowest eigenvalues are different by many orders of magnitude. Therefore, one can conclude that the reason why there exist some numerical errors is due to the bad invertibility of the Fisher matrix.

Final conclusion. From the plots, the errors corresponding to f_0 and $\Delta\Phi$ are much smaller in ET's case, to the order of 10 times smaller than advanced LIGO's results. This means that Einstein Telescope will be able to detect phase shifts that might not be observable by current interferometers. Plots also show that these phase shifts will be more easily detectable for lower resonant frequencies, and for higher phase shifts, due to the fact that rms errors are much lower. As a consequence, the minimum detectable values of $\Delta\Phi$ are smaller.

Regarding the numerical errors that arise in the cases of Einstein Telescope, one way to solve the difficulties in the inversion of the Fisher matrix could be multiplying the matrix by a certain constant to make the eigenvalues more similar, but this is left for future work.

Bibliography

[1] C.Van Den Broeck, *Gravitational Waves lecture notes* (2018).

[2] K.G. Arun, Bala R Iyer, B.S. Sathyaprakash, and Pranesh A Sundararajan, *Parameter estimation of inspiralling compact binaries using 3.5 post-Newtonian gravitational-wave phasing: The non-spinning case* (2018).

[3] M. Maggiore, *Gravitational Waves*, Oxford University Press, New York, p. 554 (2008).

[4] P. Balachandran and Ã.Ã. Flanagan, *Detectability of Mode Resonances in Coalescing Neutron Star Binaries*, Laboratory of Elementary Particle Physics, Cornell University, Ithaca, NY 14853, USA (2017).

[5] P. Ajith, *Adressing the spin question in gravitational-wave searches: Waveform templates for inspiralling compact binaries with nonprecessing spins*, LIGO laboratory, California Institute of Technology, Pasadena, CA 91125, USA and Theoretical Astrophysics, Californa Institute of Technology, Pasadena, CA 91125, USA.

[6] Ã.Ã. Flanagan and Ã.Racine, *Gravitomagnetic resonant excitation of Rossby modes in coalescing neutron star binaries*, Center for Radiophysics and Space Research, Cornell University, Ithaca, New York, 14853 and Theoretical Astrophysics, Californa Institute of Technology, Pasadena, CA 91125, USA.